400-900 nm Light Emitting Silicon Nanoparticles

R. W. Liptak*, X. D. Pi**, U. Kortshagen**, and S. A. Campbell*

*Department of Electrical and Computer Engineering, University of Minnesota
200 Union Street SE, Minneapolis, MN, USA, lipt0010@umn.edu
**Department of Mechanical Engineering, University of Minnesota
111 Church Street SE, Minneapolis, MN, USA, xdpi@me.umn.edu

ABSTRACT

A novel process has been developed to create silicon nanoparticles (Si-NPs) that emit controlled colors from blue to the near infrared. The emission is reasonably stable in air. This is the first ever report of a process that can produce the full spectrum of visible light from silicon and the first process that creates air-stable blues, greens, and yellows. The particles are created in a nonthermal silane plasma and the resultant aerosol is sent to a second plasma. The process in this chamber involves simultaneously etching and passivating the nanoparticles using a CF_4 plasma. The plasma leaves a coating on the surface that prevents the formation of Si=O bonds that are typically seen after air exposure.

Keywords: silicon, nanoparticle, passivation, light, emission

1 INTRODUCTION

Progress has recently been made in finding ways to realize efficient light emission from Si at room temperature. One of the most successful methods is to take advantage of the quantum confinement effect of Si nanoparticles (Si-NPs) with a size (i.e., diameter) < ~ 5 nm [1-8]. Several different techniques have been used to fabricate Si-NPs [3, 5-8]. The emission of light from Si-NPs in the range from near infrared to orange has been demonstrated by most of the approaches. It has been suggested that the shorter wavelength (from yellow to blue) emission is usually hampered by the oxidation of Si-NPs. This is the result of a formation of a Silicon-Oxygen double bond (Si=O) at the surface which pins the PL in the red [4]. A few wet chemistry approaches have overcome this problem by passivating the Si-NP surface, but the PL degrades quickly in air and does not produce Si-NPs that emit in the longer wavelength range [9-10].

This paper reports a novel two-stage (growth-etching/passivation) non-thermal plasma system, which provides great freedom in the control of Si-NP sizes and the in-flight modification of Si-NP surface such that the light emission from Si-NPs in the range from near infrared to blue is achieved in spite of air exposure. The main gases utilized in the system are SiH_4 for the growth of Si-NPs and CF_4 for the etching and passivating of Si-NPs, both of which are routinely employed in Si-based microelectronic industry. XPS and FTIR data shows the presence of Si-F, Si-O-F, Si-OH, and other groups on the surface. The PL wavelength is continuously tuned by changing the NP size, except for blue light emission which may result from defects on the surface of the nanoparticle. Quantum efficiency is the highest for long wavelength emitting Si-NPs. The emission is stable in air for months. Compatibility with Si microelectronic technology should facilitate the realization of the full potential of Si-NPs in applications such as display, solid-state lighting and optoelectronic integration.

2 EXPERIMENTAL

Figure 1 schematically shows our system for the synthesis [8] and dry etching of Si-NPs. A gas mixture of SiH_4/He (5%/95% in volume) and Ar was introduced into the plasma I area (a 7-inch-long quartz tube with 1/4-inch inner diameter and 3/8-inch outer diameter), immediately after which CF_4 gas was added. The flow rates of SiH_4/He were in the range from 3 to 5.5 sccm (standard cubic centimeter). Ar entered the plasma I area at a flow rate of 50 sccm. The flow rates of CF_4 were 1.5 – 3.5 sccm. The H_2 flow rate into plasma II was fixed at 6 sccm. The pressures in the plasma I area and plasma II area (a 10.5-inch-long quartz tube with 7/8-inch inner diameter and 1-inch outer diameter) were ≈ 3.8 and 0.3 Torr, respectively. Both plasmas were generated with 13.56 MHz power sources through matching networks. The power coupled into plasma I was adjusted to be slightly smaller than the critical value for the transition from diffusive plasma to constricted plasma, and was 20 - 50 W. The power coupled into plasma II was in the range from 15 to 45 W, where diffusive plasma was always obtained. Si-NPs were collected on a stainless steel filter placed behind plasma II.

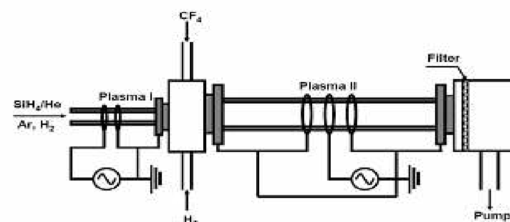

Figure 1. Synthesis and Dry Etching System Schematic

3 RESULTS

3.1 Surface Passivation

Si-NPs were characterized with X-ray photoelectron spectroscopy (XPS, Physical Electronics Inc. Model 550) and the attenuated total reflection (ATR) mode of Fourier transform infra-red spectroscopy (FTIR, Nicolet Instrument Corp. Magna-IR 750). The results are presented in figure 2. The XPS peaks are marked according to the binding energies of electrons in the outermost orbitals of various elements (Figure 2(a)). Besides Si, O is observed at the surface of Si-NPs synthesized with only plasma I (curve A in Figure 2(a)). This is consistent with the easy oxidation of Si-NPs in air. The small peak associated with C in the curve A of Figure 2(a) is due to the carbon contamination in air [11] or due to the carbon content in the stainless steel mesh that is used to collect the NP sample. After treated in the CF_4-based plasma (plasma II) there is both F and C at the surface of Si-NPs (curve B in Figure 2(a)). In the mean time the signal from O is still observed. The activation energy of 0.34 eV for oxygen diffusion in fluorocarbon materials is rather small [12]. Oxygen may easily permeate the fluorocarbon films and oxidize the underlying Si-NPs in air at room temperature even if there is a considerable fluorocarbon-film coating. This is evidenced by the stretching mode of Si-O-Si at 1074 cm^{-1} (curve B in Figure 2(b)) [13]. There are also peaks at 885 and 841 cm^{-1} for Si-NPs synthesized with only plasma I (curve A in Figure 2(b)). They are associated with oxidized Si-H groups [14]. Clearly, O is incorporated in Si-Si back bonds, giving rise to the peak at 1074 cm^{-1}. Figure 2(c) shows the deconvoluted FTIR spectrum in the range 680 – 980 cm^{-1} for Si-NPs synthesized with both plasmas I and II. Besides the peak at 885 cm^{-1} three other peaks are identified at 726, 795 and 913 cm^{-1}. They originate from the bending mode of CF_2 [15], the stretching mode of Si-C [16] and the stretching mode of Si-F [17], respectively. There are stretching modes of fluorocarbon bonds in the range from 1060 to 1220 cm^{-1} [18]. This leads to the broadened peak and shoulder around 1074 cm^{-1} for Si-NPs synthesized with both plasmas I and II (curve B in Figure 2(b)).

The XPS and FTIR measurements demonstrate that the CF_4-treated Si-NPs are passivated by O, H, C and F in contrast to only O and H for those encapsulated by natural oxide formed in air. It is known that the effect of C and F on the bandgap of Si-NPs (thus their PL energy) is much weaker than that of O [19]. Our present work further indicates that C and F may play a role in preventing the formation of oxygen-related intra-bandgap energy levels, which usually result in the absence of short-wavelength light emission from Si nanocrystals [4, 19]. However, it is important to note that besides the fluorocarbons created by the etching process, the plasma may also be forming Si-C surface films (shells) or even SiC nanoparticles. It is evident from the FTIR spectra above that Si-C bonds exist in these CF_4 treated Si-NPs. Even with high resolution XPS is difficult to properly classify the surface chemistry of the CF_4 treated Si-NPs and thus these results are not sufficient to distinguish between a Si/SiC core/shell and a Si-NP with a surface layer of chemically bonded F and C.

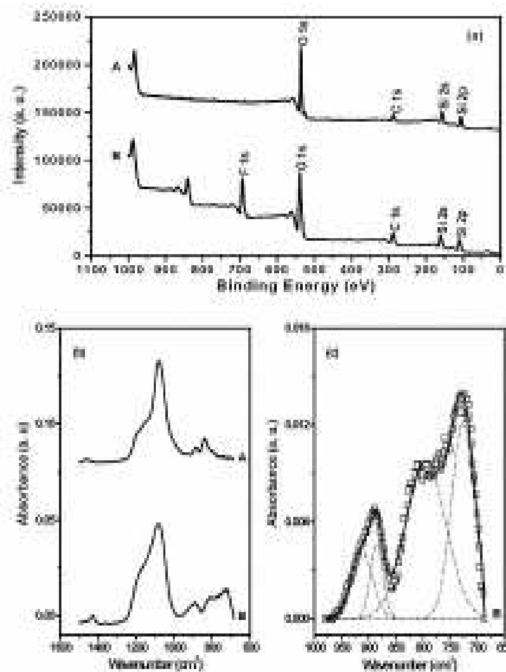

Figure 2. XPS and FTIR of Si-NPs. (a) XPS spectra from untreated (A) and CF_4 treated (B) Si-NPs. (b) FTIR results from untreated (A) and CF_4 treated (B) Si-NPs. (c) Deconvolution of the FTIR spectrum for CF_4 treated Si-NPs.

3.2 Optical Characterization

The photoluminescence (PL) from Si-NPs was measured on a Spex Fluorolog-2 spectrofluorometer with an excitation wavelength of 325 nm from a Xe lamp. A 385 nm long-pass filter was used in front of the input slit of the detection monochromator in all the PL measurements. Figure 3 shows the normalized PL spectra for Si-NPs synthesized with only plasma I (Figure 3(a)) and both plasmas I and II (Figure 3(b) and 3(c)). The production and crystallinity of the Si-NPs has been verified by means of high-resolution transmission electron spectroscopy (FEI Tecnai G2 30 HR-TEM) which is not shown here. The PL from Si-NPs synthesized with only plasma I blueshifts from 686 to 666 nm when the flow rate of SiH_4/He changes from 5.5 to 3 sccm (for clarity the data for the flow rates of 4.5 and 4.0 sccm is not shown in Figure 3(a)). Using a modified equation [7, 20] for the relation between PL energy and Si-NPs size in the quantum confinement model, we calculate that the size of Si-NPs correspondingly changes from 3.57 to 3.40 nm. These NP sizes approximate

those observed in HR-TEM. The partial pressure of SiH_4 in plasma I decreases with the decrease of SiH_4/He flow rate in the present experimental setup. This agrees with previous work [8] which has shown that Si-NPs size is proportional to the partial pressure of SiH_4.

When Si-NPs pass through plasma II red-light-emitting Si-NPs produced in plasma I are etched. The etching is achieved by the reaction between Si-NPs and free F radicals in plasma II, resulting in the formation of the volatile gas SiF_4 [21]. Figure 3(b) illustrates the PL spectra for Si-NPs etched with a CF_4 flow rate of 1.5 sccm after synthesized in plasma I with various SiH_4/He flow rates. It is clear that the light emission blueshifts with the decrease of SiH_4/He flow rate, as seen in Figure 3(a). Thus, after the same etching plasma, the size of Si-NPs is depends on their pre-etching size. From the PL peaks at 591, 576, 566 and 531 nm we obtain that the sizes of Si-NPs are approximately 2.86, 2.76, 2.70 and 2.48 nm, respectively. Figure 3(c) demonstrates the effect of CF_4 flow rate on the etching of Si-NPs, which are produced with a SiH_4/He flow rate of 3 sccm. As the flow rate of CF_4 changes from 1.5 to 3.5 sccm, the PL peak redshifts from 531 to 572 nm, respectively. The corresponding changes in the size of Si-NPs are from approximately 2.48 to 2.73 nm. It is known [22] that the increase of CF_4 flow rate gives rise to an enhanced production rate of CF_2 radicals, which are the dominant precursors of low volatility fluorocarbon films formed on Si surface. These films are responsible for the suppression of Si etching. Therefore, in plasma II the etching is attenuated when the flow rate of CF_4 increases.

It is interesting to note that there exists a clear blue light emission band around 400 nm in the PL spectra for Si-NPs $< \sim 2.73$ nm (PL peak at 572 nm) shown in both Figure 3(b) and 3(c). In fact, the blue light emission band does not disappear even for those Si-NPs depicted in Figure 3(a). The ratio of the blue light emission intensity to the longer-wavelength emission intensity decreases with the increase of Si-NP size. This causes the apparent disappearance of the blue light emission band in the PL spectra for Si-NP $>$ 2.73 nm. Several research groups have claimed that blue light emission from Si-NPs synthesized in solutions originates from direct-bandgap transition [6]. Theoretical work has shown that the direct-bandgap of Si nanocrystals widen with the decrease in size [23]. Since the position of the blue light emission band does not change with the size of Si-NPs in the present work, the above-mentioned claim should not apply. An effect called self-purification mechanism leads to the tendency for defects and impurities to reside on the surface of the nanoparticles [24]. Both non-radiative and radiative states may derive from these defects and impurities. The position of the blue light emission band was found to be around 395 nm by removing the optical filter, which causes an artifact in the spectral range below 400 nm. The energy of the blue light emission and the shape of the blue light emission band are similar to those obtained from oxidized porous Si [25] or oxidized organically grafted Si nanocrystals [26]. It is likely that oxidation-induced defects are formed at the surface of Si-NPs when they are oxidized in air. The radiative states related to these defects are mainly responsible for the blue light emission band [25]. For defects located in the oxide their concentration is proportional to the oxide volume, which is proportional to the size of Si nanocrystals [7]. Hence, if the defects responsible for the blue emission band are located in the oxide, their concentration would decrease with the decrease of Si-NP size. This would lead to weaker blue light emission when Si-NPs become smaller, which is not the case in the present work. Therefore, the oxidation-induced defects giving rise to the blue light emission band should be located at the NP/oxide interface.

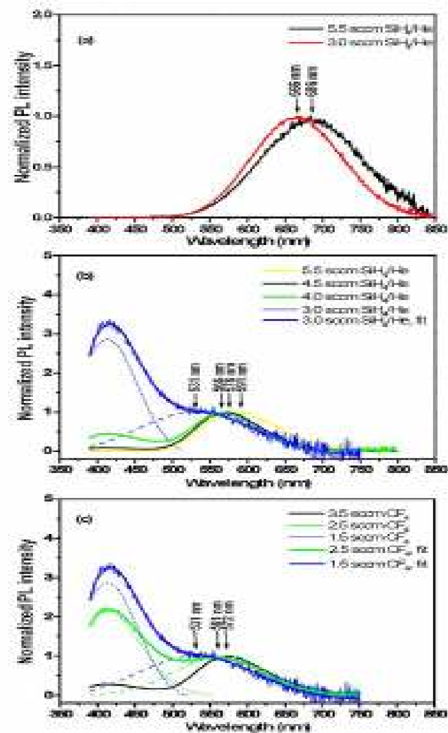

Figure 3. Normalized PL spectra for Si-NPs. (a) Plasma I only. (b) Second plasma added with a CF_4 flow rate of 1.5 sccm for various SiH_4/He flow rates. (c) Both plasmas used. The flow rate of SiH_4/He was 3 sccm for various CF_4 flow rates. Dashed lines in (b) and (c) indicate two constituent peaks.

The integrated two-stage plasma system allows the production of Si-NPs that emit light in the full visible spectrum. Figure 4 shows a photo of the deep red (740 nm), red-orange (675 nm), yellow (592 nm), green (572 nm) and blue (441 nm) emissions from Si-NPs under the illumination of an ultraviolet (UV) lamp. The radiation of the UV lamp is centered at 365 nm. A 385 nm short-pass filter was placed between the UV lamp and each sample.

It is important to note that the CF_4 particles are extremely stable in air. All the Si-NP samples in Figure 4 are more than one week old.

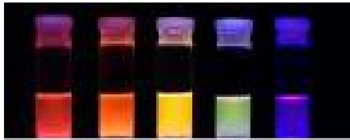

Figure 4. Luminescent Si-NPs

The PL of the Si-NPs changes slowly with time until it saturates. Generally, the shorter wavelength emission has larger shifts that the longer wavelength emission. This is representatively illustrated in Figure 5 by the data for Si-NPs which originally emitted light at a wavelength of ~ 579 nm.

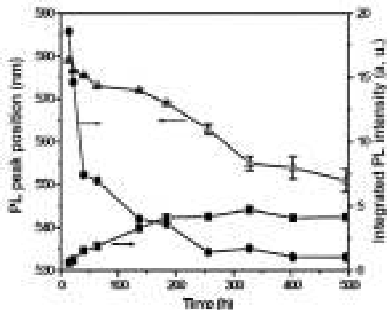

Figure 5. Change of PL from Si-NPs with time. Δ: peak position of the longer-wavelength light emission. ●: intensity of the longer-wavelength light emission. ■: intensity of emission in the blue band. Si-NPs were excited at 325 nm.

With the increase in time the PL blueshifts. After ~ 12 days the blueshift of PL stops. The PL finally peaks at ~ 553 nm. This kind of change in the PL has been previously demonstrated in the study of Si nanocrystals > 3 nm [27]. The underlying mechanism is the self-limiting oxidation of nanometer-sized Si [28]. When Si nanocrystals are oxidized, the crystalline cores shrink. The resultant reduction of Si nanocrystal size leads to the blueshift of PL according to the quantum confinement effect.

4 CONCLUSIONS

Si-NPs that emit light in the full visible spectrum have been synthesized with an all gas-phase approach at high production yields. With the possible exception of blue light emission, the light from Si-NPs agrees with the quantum confinement effect and is generally stable in air. This work was supported by NSF under MRSEC grant DMR0212302. This work was performed at the Minnesota Characterization Facility which receives support from NSF through NNIN.

REFERENCES

[1] P. M. Fauchet, Topics in Appl. Phys. 94, 177, 2004.
[2] L.T. Canham, Appl. Phys. Lett. 57, 1046, 1990.
[3] L. Pavesi, L. Dal Negro, C. Mazzoleni, G. Franzò and F. Priolo, Nature 408, 440, 2000.
[4] M. V. Wolkin, J. Jorne, P. M. Fauchet, G. Allan, and C. Delerue, Phys. Rev. Lett. 82, 197, 1999.
[5] Z. H. Lu, D. J. Lockwood, and J. –M. Baribeau, Nature 378, 258, 1995.
[6] J. P. Wilcoxon, G. A. Samara, and P. N. Provencio, Phys. Rev. B 60, 2704, 1999.
[7] G. Ledoux, O. Guillois, D. Porterat, C. Reynaud, F. Huisken, B. Kohn, and V. Paillard, Phys. Rev. B 62, 15942, 2000.
[8] L. Mangolini, E. Thimsen, and U. Kortshagen, Nano Lett. 5, 655, 2005.
[9] X. G. Li, Y. Q. He, S. S. Talukdar, and M. T. Swihart, Langmuir 19, 8490, 2003.
[10] D. Jurgergs, E. Rogojina, L. Mangolini, and U. Kortshagen, Appl. Phys. Lett. 88, 233116, 2006.
[11] G. S Oehrlein, R. M. Tromp, J. C. Tsang, Y. H. Lee, and E. J. Petrillo, J. Electrochem. Soc. 132, 1441, 1985.
[12] W. J. Koros, J. Wang, and R. M. Felder, Appl. Polym. Sci. 26, 2805, 1981.
[13] P.G. Pai, S. S. Chao, Y. Takagi, and G. Lucovsky, J. Vac. Sci. Technol. A 4, 689, 1986.
[14] G. Lucovsky, J. Yang, S. S. Chao, J. E. Tyler, and W. Czubatyj, Phys. Rev. B 28, 3225, 1983.
[15] Y. Xin, Z. Y. Ning, C. Ye, S. H. Xu, J. Chen, and X. H. Lu, Thin Solid Films 472, 44, 2005.
[16] A. J. Steckl, J. Devrajan, C. Tran, and R. A. Stall, Appl. Phys. Lett. 69, 2264, 1996.
[17] S. –K. JangJian and Y. –L. Wang, Surf. Coat. Technol. 200, 3140 2006.
[18] M. Bertino, A. Corazza, M. Martini, A. Mervic, and G. Spinolo, J. Phys.: Condens. Matter 6, 63454352, 1994.
[19] A. Puzder, A. J. Williamson, J. C. Grossman, and G. Galli, Phys. Rev. Lett. 88, 097401, 2002.
[20] C. Delerue, G. Allan, and M. Lannoo, Phys. Rev. B, 48, 11024, 1993.
[21] J. D. Plummer, M. D. Deal, and P. B. Griffin, "Silicon VLSI technology fundamentals, practice and Modeling," Prentice Hall, 2000.
[22] G.S. Oehrlein and H. L. Williams, J. Appl. Phys. 62, 662, 1987.
[23] Z. Y. Zhou, L. Brus and R. Friesner, Nano Lett. 3, 163, 2003.
[24] G. M. Dalpian and J. R. Chelikowsky, Phys. Rev. Lett. 96, 226802, 2006.
[25] D. I. Kovalev, I. D. Yaroshetzkii, T. Muschik, V. Petrova-Koch, and F. Koch, Appl. Phys. Lett. 64, 214, 1994.
[26] F. J. Hua, F. Erogbogbo, M. T. Swihart, and E. Ruckenstein, Langmuir 22, 4363, 2006.
[27] G. Ledoux, J. Gong, and F. Huisken, Appl. Phys. Lett. 79, 4028, 2001.
[28] H. I. Liu, D. K. Biegelsen, F. A. Ponce, N. M. Johnson, and R. F. W. Pease, Appl. Phys. Lett. 64, 1383, 1994.